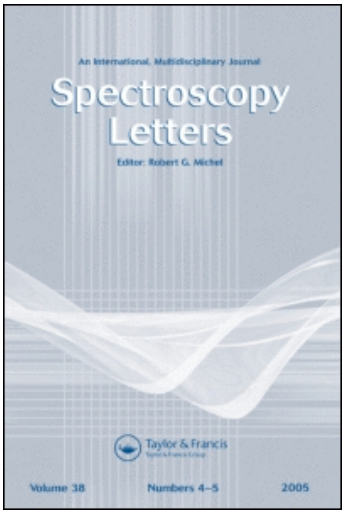

Spectroscopy Letters
Publication details, including instructions for authors and subscription information:
http://www.informaworld.com/smpp/title~content=t713597299

Quantitative Analysis of Added Ammonium and Nitrate in Silica Sand and Soil Using Diffuse Reflectance Infrared Spectroscopy

Suwanee Boonmung[a]; Mark R. Riley[a]
[a] Department of Agricultural and Biosystems Engineering, The University of Arizona, Tucson, AZ, USA

Online publication date: 08 July 2003

To cite this Article Boonmung, Suwanee and Riley, Mark R.(2003) 'Quantitative Analysis of Added Ammonium and Nitrate in Silica Sand and Soil Using Diffuse Reflectance Infrared Spectroscopy', Spectroscopy Letters, 36: 3, 251 — 274
To link to this Article: DOI: 10.1081/SL-120024358
URL: http://dx.doi.org/10.1081/SL-120024358

SPECTROSCOPY LETTERS
Vol. 36, No. 3, pp. 251–274, 2003

Quantitative Analysis of Added Ammonium and Nitrate in Silica Sand and Soil Using Diffuse Reflectance Infrared Spectroscopy

Suwanee Boonmung and Mark R. Riley*

Department of Agricultural and Biosystems Engineering,
The University of Arizona, Tucson, Arizona, USA

ABSTRACT

Diffuse reflectance infrared Fourier transform spectroscopy (DRIFTS) in both near infrared (NIR) and mid infrared (MIR) has been previously shown to be effective in quantifying soil nitrogen concentrations when calibrated using numerous field soil samples. However, such an approach incorporates samples that may contain substantial correlations between physical and chemical properties. To address these concerns, the performance of DRIFTS coupled with PLS regression in NIR regions, 5000–4000 cm^{-1} (2000–2500 nm) and 6500–5500 cm^{-1} (1540–1820 nm), and the MIR region, 3400–2400 cm^{-1} (2940–4170 nm), was assessed through analysis of the concentration of ammonium (NH_4^+) (0–50 ppm) and nitrate (NO_3^-) (0–200 ppm) artificially incorporated

*Correspondence: Mark R. Riley, Department of Agricultural and Biosystems Engineering, The University of Arizona, Shantz Bldg., Room 403, Tucson, AZ 85721, USA; E-mail: riley@ag.arizona.edu.

DOI: 10.1081/SL-120024358
0038-7010 (Print); 1532-2289 (Online)

www.dekker.com

MARCEL DEKKER, INC.
270 Madison Avenue, New York, New York 10016

into a series of silica sand samples with a consistent particle size. The influence of different particle sizes of sand was also analyzed quantitatively. The Pima clay loam soil was then evaluated with concentration ranges of 0–200 ppm NH_4^+ and 180–1000 ppm NO_3^- added to the soil samples. With sand samples, accurate NH_4^+ measurements could be performed using all three ranges. The MIR region was significantly more useful for NO_3^- measurement than those of NIR regions. The MIR region also performed reasonably well with soil samples but both NIR regions provided poor results. The detection limits for NH_4^+ and NO_3^- measurements in sand were 9 ppm NH_4^+ and 39 ppm NO_3^- with the correlation coefficients (R^2) of roughly 97% and 96%, respectively, and in soil were 100 ppm NH_4^+ and 330 ppm NO_3^- with the correlation coefficients (R^2) of roughly 80% and 90%, respectively.

Key Words: DRIFTS; Mid infrared; Near infrared; Ammonium; Nitrate; Sand; Soil.

INTRODUCTION

The nitrogen (N) requirement for many agricultural crops is usually very high, thus necessitating the use of fertilizers. The excessive use of N fertilizer in many regions, particularly those with N poor soils, has raised concern about groundwater contamination. This has led to the increasing need for improved fertilization management practices, which require rapid and accurate techniques for determination of N in soils. Such addition aids farmers in applying adequate amounts of N fertilizer at precise times and locations.

Nitrogen occurs in both organic and inorganic fractions of soil. The organic soil N occurs largely as NH_2 groups while the inorganic soil N primarily occurs as nitrate (NO_3^-) and ammonium (NH_4^+).[1] The levels of N in a soil sample are usually quantified through destructive methods by which the sample is extracted or digested to convert N into detectable forms. These methods are laborious and expensive, thus restricting the number and frequency of samples that can practically be applied to characterize the N content of a sizeable agricultural field. Spectroscopic measurement provides a potentially inexpensive and rapid alternative that could provide more timely information on soil composition.

Diffuse reflectance infrared Fourier transform spectroscopy (DRIFTS) has been used as a rapid and nondestructive method for both qualitative and quantitative analysis of soil properties. DRIFTS involves measurement of the flux per wavelength of light reflected in a scattered manner from a

sample. The relationship between DRIFTS spectra and analyte concentration is nonlinear, thus data transformations such as Kubelka–Munk (K–M) or log (1/R), where R is the ratio of sample reflectance spectrum to the reflectance of the nonabsorbing standard such as KBr, are commonly used to linearize this relationship. In general, the K–M function would be useful for an analyte with low absorptivity and low concentration surrounded by a non-absorbing matrix while the log ($1/R_\infty$) format would provide more linearity than the K–M function when the sample matrix is strongly absorbing such as found with soil matrices. Multivariate regression techniques such as multiple linear regression (MLR) and partial least squares (PLS) regression are used to compensate for the nonlinearity between analyte concentration and the transformed spectral data.

Soil organic and inorganic compounds have distinct features in both the NIR region, 10000–4000 cm^{-1} (1000–2500 nm), and the MIR region, roughly 4000–200 cm^{-1} (2500–50000 nm). The free NH_4^+ ion exhibits infrared active fundamental bands near 1400 cm^{-1} (7100 nm) and 3150 cm^{-1} (3200 nm) and overtone and combination bands are located near 2840 cm^{-1} (3500 nm), 3020 cm^{-1} (3300 nm), 5000 cm^{-1} (2000 nm), and 6600 (1500 nm).[2,3] The NO_3^- ion has infrared active fundamental bands around 720 cm^{-1} (13900 nm), 830 cm^{-1} (12000 nm), and 1390 cm^{-1} (7200 nm) and overtone and combination bands locate near 1790 cm^{-1} (5600 nm), 2430 cm^{-1} (4100 nm), 2800 cm^{-1} (3600 nm), and 5200 cm^{-1} (1900 nm).[4,5]

The NIR and MIR regions within the ranges of 6000–4000 cm^{-1} (1700–2500 nm) and 4000–400 cm^{-1} (2500–25000 nm) have been used for the determination of soil total N and mineral N concentrations. Janik et al.[6] have summarized the applicability of DRIFTS to analyze soil chemical and physical properties. Quantitative analysis of some soil properties that are relatively high in concentration and correlated to the chemistry of the soil matrix such as total N and total organic carbon have been effectively reported using DRIFTS.[4,7–12] The prediction of total N in different field soils has been reported with high correlation coefficients (R^2>80%) and somewhat low standard errors of prediction (SEP<300 ppm) with the average concentration of approximately 3000 ppm. Plants take up N in the form of NH_4^+ or NO_3^-, depending upon soil conditions,[1] and so it is more valuable to know the concentration of individual N species than for total N alone. At this time few studies[4,10] have reported the evaluation of DRIFTS for the determination of soil mineral N such as NH_4^+ and NO_3^-. This lack of attention may be due to the low concentration of each species (usually less than 50 ppm without N fertilizers) or to the temporal changes in the relative levels of each through the nitrification process.

For quantitative analysis of soil N, the DRIFTS method is usually calibrated with classical laboratory methods; thus, its ability depends upon the accuracy of the calibrated techniques and the statistical and mathematical groups used. Soil is complex both physically and chemically with multiple attributes that may vary in samples collected in the same field. When DRIFTS is calibrated using field soil samples, physical attributes of the soil such as texture, particle size distribution, and water content could substantially affect the absorptivity and scattering properties of the sample matrix, and thus enhance the nonlinearity of the DRIFTS technique. The suitable vibrational features for soil N are difficult to obtain as they are overlapped or interfered by major soil components such as sand (quartz) and water. Previous studies have not performed N measurements with collections of samples having minimal physical variations. As soil types vary from study to study, the physical variations also likely vary, thus measurement capabilities depend on more than just chemical variations.

Since variations in field soil samples can have several effects on the capability of DRIFTS for soil N quantification, there can be benefits from studying the capability of this method to quantify N compounds in soil matrices with constant physical characteristics. The overall objective of this study is to evaluate the feasibility of utilizing DRIFTS method together with PLS regression to perform chemical analyses of soil NH_4^+ and NO_3^- while maintaining consistent physical properties of soil. This will be accomplished by studying silica sand (the major component of soil) to which have been added known and varying amounts of important N sources (NH_4Cl, $NaNO_3$ and NH_4NO_3). The particle sizes of sand were reduced to quantitatively investigate the effect of physical variations of sand while keeping similar N components. Then a neat soil sample was investigated to validate the optimal calibration model developed using the previous sand matrices.

EXPERIMENTAL

Acid washed sand (quartz) with the particle size range of 212–300 μm (#70–50 U.S. Mesh) served as the sample matrix. To this was added random but known amounts of N (NH_4Cl, $NaNO_3$, and NH_4NO_3) to yield at least 40 samples with independent amounts of each N component. Seven experimental groups were examined in this study. Table 1 summarizes the type of N source used, the concentration ranges of NH_4^+ and NO_3^-, and the number of samples for each group. Briefly, the N concentrations varied from 0 to 50 ppm and from 0 to 200 ppm for NH_4^+ and NO_3^- in sand samples, respectively. These concentrations are appropriate for arid soils in

Table 1. Summary of all groups of nitrogen sources added onto silica sand.

Group[a]	Nitrogen source	Particle size (μm)	# of samples	Concentration range (ppm w w^{-1})	
				NH_4^+	NO_3^-
No. 1	NH_4Cl	212–300	40	0–50	–
No. 2	$NaNO_3$	212–300	40	–	0–200
No. 3	$NH_4Cl+NaNO_3$	212–300	51	0–50	0–200
No. 4	NH_4NO_3	212–300	40	0–60	0–200
No. 5	$NH_4Cl+NaNO_3$	63–106	20	0–50	0–200
No. 6	$NH_4Cl+NaNO_3$	Less than 53	20	0–50	0–200
No. 7	$NH_4Cl+NaNO_3$	Less than 2000	100	0–200	180–1000

[a]The silica sand samples served as the sample matrices in Groups No. 1 to 6 while soil samples were used in Group No. 7.

Arizona. For Groups No. 5 and 6, the initial sand particles (212–300 μm) were ground and sieved to yield the sand particle sizes of 63–106 μm (#230–140 U.S. Mesh) and less than 53 μm (less than #270 U.S. Mesh), respectively. N was added to sand by preparing a liquid solution of each N source in water (pH=6.0), which was mixed with sand. This approach yielded samples which were more homogeneous than those prepared by addition of powders. The powered sand samples, roughly 280 mg, were placed into sampling cups (10mm in diameter and 2.3mm in depth) and volumes of N solutions were pipetted onto the sand so as to avoid losses due to transfer. Each sample received the same amount of water to consistently distribute N sources to the whole sand sample in the cups. Samples were air-dried in a desiccator for 24 hours before spectra were collected. Sand samples were scanned without dilution with powdered KBr.

The Pima Clay Loam soil (Typic Torrifluvent) collected from the Marana Agricultural Center, The University of Arizona, Tucson, Arizona, was air-dried and sieved to obtain a particle size of less than 2000 μm. This soil sample originally contained approximately 180 ppm NO_3^- and 0 ppm NH_4^+. Initial studies (data not shown) indicated that the NH_4^+ and NO_3^- features were overlapped by other components in soil samples when using a neat (undiluted) soil sample added with the previous N concentration ranges (0 to 50 ppm NH_4^+ and 0 to 200 ppm NO_3^-). Thus relatively high contents of NH_4^+ and NO_3^- in soil samples (0 to 200 ppm NH_4^+ and 180 to 1000 ppm NO_3^-) were investigated to determine the detection limit of the DRIFTS method using soil samples. Soil samples were also added with known but random amounts of NH_4Cl and $NaNO_3$ solutions. The 1 wt%

MARCEL DEKKER, INC.
270 Madison Avenue, New York, New York 10016

powdered soil sample was mixed with KBr powder using a Wig-L-Bug grinder for approximately 30 seconds before being transferred to a sampling cup and scanned with DRIFTS equipment.

To verify NH_4^+ and NO_3^- concentration in the sand samples, traditional chemical methods were employed. An ammonia electrode (Model 95-12, Orion Research, Inc., Beverly, MA) was used to measure NH_4^+ in selected sand samples. A colorimetric analysis with chromotropic acid (CTA)[13] was utilized to determine NO_3^- contents. These reference measurements were performed after sample spectra were collected. In all cases, the measured and expected concentrations were nearly the same, within the detection limit of each assay, approximately 5% (data not shown).

Spectra were collected on a Nicolet Magna 560 Fourier Transform Infrared (FTIR) spectrometer (Thermo Nicolet Corporation, Madison, WI) equipped with the Wilmad 148-1-Diffuse Reflectance Accessory (Wilmad Glass Company, Inc., Buena, NJ), a 50 W Tungsten source, CaF_2 beamsplitter, and liquid nitrogen-cooled InSb detector. Sample cups were inserted into the sample holder and placed into the DRIFTS accessory. A DRIFTS spectrum was produced by ratioing the sample spectrum to the background spectrum of powdered KBr. The log (1/R) format was used to produce absorbance spectra. Each spectrum consisted of 256 co-added triangularly apodized scans collected from 10,000–2100 cm^{-1} (1000–4760 nm) at 2-cm^{-1} resolution. Triplicate spectra were collected successively for each sample, yielding a total number of spectra of 120 for 40 samples. A background spectrum of KBr was collected after every fifth sample.

Two NIR spectral regions and one high-wavenumber region of the MIR were isolated and analyzed for both NH_4^+ and NO_3^- prediction. These regions were 5000–4000 cm^{-1} (2000–2500 nm), 6500–5500 cm^{-1} (1540–1820 nm), and 3400–2400 cm^{-1} (2940–4170 nm), respectively. These spectral regions are located between the strong water absorbance features located around 7100 cm^{-1} (1330 nm), 5380 cm^{-1} (1860 nm), 3750 cm^{-1} (2670 nm), and 1630 cm^{-1} (6140 nm).[14] Partial least squares (PLS-1) regression analysis software, operated on a Silicon Graphics O_2 workstation, was employed to correlate N concentrations to spectral features. This software was developed and provided by Professor Gary Small from the Center for Intelligent Chemical Instrumentation in the Department of Chemistry at Ohio University. Spectral data were mean-centered and no other mathematical pretreatments were performed. The optimal spectral ranges and the number of PLS factors used in the calibration model were determined based on cross-validation procedures. Approximately two-thirds of spectra were randomly placed into calibration data sets and the rest of spectra were included in prediction sets. The samples with the highest and lowest concentration were always placed in the calibration set and replicate

spectra were always placed into the same sample set. This analysis was performed in triplicate as to minimize sample dependent effects.

A C-shell computer script was operated on a Silicon Graphics O_2 workstation to investigate a variety of possible combinations of model parameters for each spectral range. The script builds calibration models with varying numbers of PLS factors from 1 to 20 and with varying spectral ranges within each isolated spectral range. This follows a modified grid search that permits the unbiased evaluation of many calibration data sets. For each model, the script searches for spectral ranges that contain significant analyte information. Standard errors of prediction values (SEP) initially are computed for 100 cm^{-1} wide regions at 100 cm^{-1} intervals. The region with the lowest SEP is assumed to contain significant analyte information and becomes the focus of further evaluation. The upper and lower values of this range are increased and subsequently decreased by a predetermined amount and the corresponding SEP values calculated. The process of modifying the maximum and minimum frequencies and evaluating ranges is repeated four times; ensuing iterations have a more narrow step change in the spectral range. The number of PLS factors is incremented and another spectral range search is implemented. The conditions found to be optimal for each PLS factor is then determined. Outlier detection is based upon leverage and residuals of individual concentration. Data in both calibration and prediction sets that exceed the cutoff values of leverage and residual are detected as outliers. The outliers that are common in most triplicate sets were removed before final analysis of data. See Martens and Naes[15] for more detailed information about PLS analysis, cross-validation methods, and outlier detection techniques.

RESULTS AND DISCUSSION

Ammonium and Nitrate Measurements in Sand Samples

As indicated in Figures 1–3, the spectral intensities of NH_4Cl are quite high relative to sand in all three regions (5000–4000 cm^{-1}, 6500–5500 cm^{-1}, and 3400–2400 cm^{-1}); thus, high PLS efficiency in predicting NH_4^+ concentrations would be expected within these three regions. The NH_4Cl spectrum exhibits many distinct features in all three regions; for example, around 2810 cm^{-1} (3560 nm), 2650 cm^{-1} (3770 nm), 4820 cm^{-1} (2070 nm), 4540 cm^{-1} (2200 nm), 6250 cm^{-1} (1600 nm), and 5970 cm^{-1} (1680 nm). The NH_4Cl features in the 6500–5500 cm^{-1} region are somewhat broader and less intense than those features in other two regions (Figure 3).

MARCEL DEKKER, INC.
270 Madison Avenue, New York, New York 10016

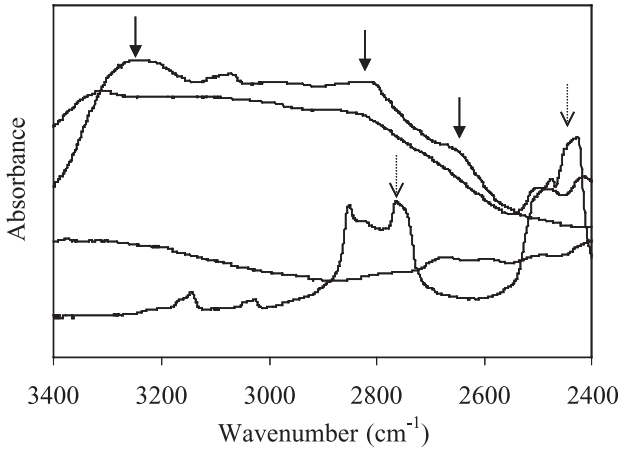

Figure 1. DRIFTS spectra of powdered samples in the region of 3400–2400 cm^{-1} indicated in decreasing order at 3000 cm^{-1} as NH_4Cl, NH_4NO_3, sand, and $NaNO_3$, respectively. The solid and dashed arrows point at the NH_4^+ and NO_3^- features respectively.

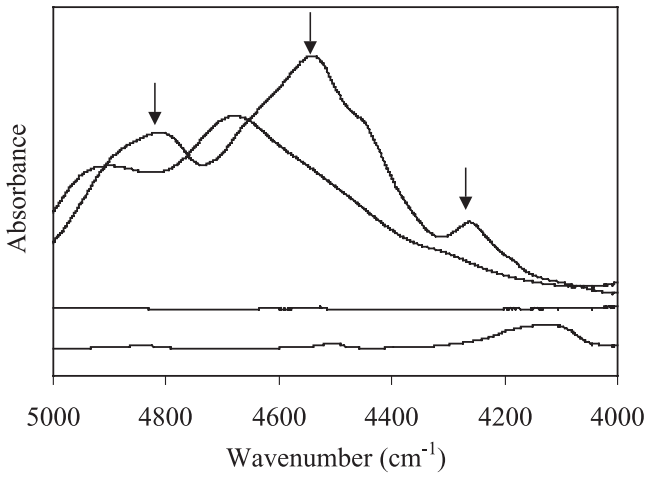

Figure 2. DRIFTS spectra of powdered samples in the region of 5000–4000 cm^{-1} indicated in decreasing order at 4400 cm^{-1} as NH_4Cl, NH_4NO_3, sand, and $NaNO_3$, respectively. The solid arrows point at the NH_4^+ features.

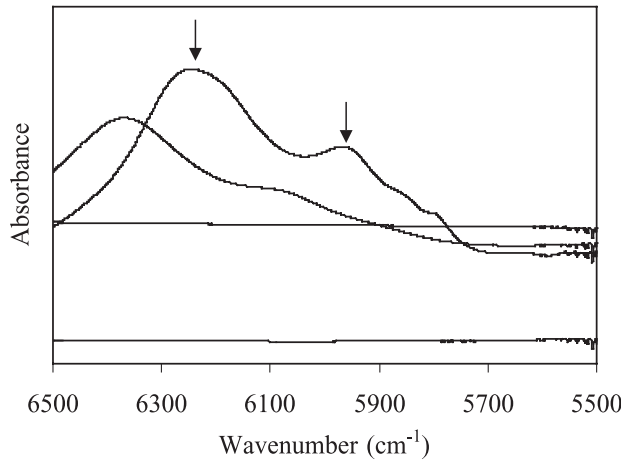

Figure 3. DRIFTS spectra of powdered samples in the region of 6500–5500 cm^{-1} indicated in decreasing order at 6100 cm^{-1} as NH_4Cl, NH_4NO_3, sand, and $NaNO_3$, respectively. The solid arrows point at the NH_4^+ features.

$NaNO_3$ has many features in the NIR region (both 5000–4000 cm^{-1} and 6500–5500 cm^{-1}) but the signal intensities are very low compared with those of sand and most likely are masked by the intense signal of sand (Figures 2 and 3). On the other hand, the absorbance intensities of some features of $NaNO_3$ in the MIR region (3400–2400 cm^{-1}) are visually more intense than those of sand (Figure 1). The $NaNO_3$ features around 2800 cm^{-1} (3600 nm) and 2500 cm^{-1} (4000 nm) are apparent within the MIR region.

The spectral features of NH_4NO_3 due to NH_4^+ in all three regions resemble the spectral features of NH_4Cl, but are shifted to high frequencies (Figures 1–3). The NO_3^- features are most apparent in the 3400–2400 cm^{-1} region. The shift of NH_4^+ features and the distinctness of NO_3^- features in the MIR region might be due to either the significantly higher spectral intensities of NH_4^+ features relative to NO_3^- features, especially in the NIR region, or to the interferences between NH_4^+ and NO_3^- features.

Table 2 shows the average PLS parameters of three independent calibration and prediction sets for NH_4^+ measurement after one outlier was removed (Group No. 1). The effective model parameters are excellent for all spectral regions. High correlation between DRIFTS spectral data and NH_4^+ concentration are achieved (R^2>94%). The SEC values are quite similar in all regions. SEP's are lowest in the 5000–4000 cm^{-1} and 3400–

Table 2. Optimal parameters and measurement errors for PLS calibrations of groups No. 1 and 2.

Spectral range (cm^{-1})	#Factors	R^2 (%)[a]	SEC (ppm)[b]	SEP (ppm)[c]	Max. concentration (ppm)[d]	Optimal range (cm^{-1})
Group No. 1: NH_4Cl						
3400–2400	3	95	2.32	1.68	43	2800–2520
5000–4000	2	96	2.28	1.73	43	4830–4470
6500–5500	3	94	2.62	2.54	43	6330–5850
Group No. 2: $NaNO_3$						
3400–2400	3	95	13.14	12.53	207	2510–2400
5000–4000	3	37	48.03	41.00	207	4310–4100
6500–5500	3	49	42.88	44.80	207	6380–6000

[a]Coefficient of determination.
[b]Standard error of calibration.
[c]Standard error of prediction.
[d]Maximum concentration of analyte in the study.

2400 cm^{-1} regions with values of roughly 2 ppm. The relatively high SEP in the 6500–5500 cm^{-1} region (approximately 2.5 ppm) might be due to the broad and low intensity features in the 6500–5500 cm^{-1} region. On the average, the coefficient of variation (CV), defined as the ratio of SEP to the total concentration ranges, for NH_4^+ determination of Group No. 1 is 5%. The number of PLS factors required is essentially the same for all three regions for Group No. 1 (Table 2). The optimal spectral ranges as indicated in Table 2 are the ranges of the most effective model, in terms of R^2, SEC, and SEP, among triplicate calibration sets. The automated grid search includes some distinct features of NH_4Cl in all three spectral regions (e.g., 2650 cm^{-1}, 4540 cm^{-1}, and 5970 cm^{-1}). Since the automated grid algorithm searches for the lowest SEP, it is possible that the selected spectral region is different in each calibration set with a small difference in SEP, especially when the analyte has many distinct features.

The optimal PLS parameters for NO_3^- prediction after six outliers were eliminated are shown in Table 2 (Group No. 2). The 3400–2400 cm^{-1} region indicates more effective PLS results than either the 5000–4000 cm^{-1} or 6500–5500 cm^{-1} regions. SEP's are 13 ppm, 41 ppm, and 45 ppm for 3400–2400 cm^{-1}, 5000–4000 cm^{-1}, and 6500–5500 cm^{-1} regions, respectively. Therefore, the 3400–2400 cm^{-1} region was used for NO_3^- determination in sand sample for the remainder of the experiments. High correlation between DRIFTS spectral data and NO_3^- concentration

are achieved (R^2=95%). The SEC and SEP values are similar, roughly 13 ppm, and the CV value is 6%. The number of PLS factors required for NO_3^- determination in Group No. 2 are the same as required for NH_4^+ determination (Table 2). The optimal spectral range (2510–2400 cm^{-1}) includes the distinct features of $NaNO_3$ that are not masked by sand within the interested concentration range. The grid search also selects other spectral ranges in which the distinct $NaNO_3$ features are still shown in sample spectra (e.g., 2900–2700 cm^{-1}).

Table 3 presents the optimal PLS parameters for NH_4^+ determination of Groups No. 3 and 4. Four outliers were removed from each group. The R^2 values are high for both groups in all regions (more than 96%). For Group No. 3, the SEC, SEP, and CV values are lowest in the 5000–4000 cm^{-1} region with values of 2.3 ppm, 2.6 ppm, and 5% respectively. The number of PLS factors required is less for the MIR region compared with both two NIR regions, requiring 3 and 5 factors, respectively. The spectral intensities of NH_4^+ features in the MIR region is stronger than those in NIR regions and thus fewer PLS factors would

Table 3. Optimal parameters and measurement errors for PLS calibrations of groups No. 3 and 4.

Spectral range (cm^{-1})	#Factors	R^2 (%)[a]	SEC (ppm)[b]	SEP (ppm)[c]	Max. concentration (ppm)[d]	Optimal range (cm^{-1})
Group No. 3: $NH_4Cl+NaNO_3$						
Nitrate measurement						
3400–2400	5	96	13.61	12.01	194	2560–2400
Ammonium measurement						
3400–2400	3	97	2.92	3.16	49	3300–3000
5000–4000	5	98	2.32	2.57	49	4520–4350
6500–5500	5	98	2.42	3.35	49	6500–5890
Group No. 4: NH_4NO_3						
Nitrate measurement						
3400–2400	5	96	10.62	13.53	215	2900–2800
Ammonium measurement						
5000–4000	5	98	2.56	2.83	63	4970–4900
6500–5500	5	98	2.24	3.05	63	6400–6100

[a]Coefficient of determination.
[b]Standard error of calibration.
[c]Standard error of prediction.
[d]Maximum concentration of analyte in the study.

be required to remove variations such as noise and spectral interferences. The optimal spectral ranges in the 3400–2400 cm^{-1} region for NH_4^+ measurement is clearly separated from the one used for NO_3^- measurement for all calibration sets (i.e., approximately divided at 2900 cm^{-1}; higher wavenumber for NH_4^+ whereas lower wavenumber for NO_3^- prediction).

Since the concentrations of NH_4^+ and NO_3^- are perfectly correlated for sand samples mixed with NH_4NO_3, the automated grid search undoubtedly selected the same spectral ranges for both NH_4^+ and NO_3^- determination. Thus, for Group No. 4, the 3400–2400 cm^{-1} region was used only for NO_3^- prediction while both 5000–4000 cm^{-1} and 6500–5500 cm^{-1} regions were used for NH_4^+ prediction. Note that the 3400–2400 cm^{-1} region could still be used for NH_4^+ measurement for Group No. 4 but both spectral ranges in NIR region would be more appropriate to find the reasonable ranges for NH_4^+ prediction that are somewhat free from NO_3^- interferences.

Despite the differences between Groups No. 3 and 4, the values of R^2, SEC, SEP, and CV are quite similar for NH_4^+ measurement, approximately 97%, 2.5 ppm, 3 ppm, and 5.5%, respectively. The number of PLS factors is similar for the determination of NH_4^+ in both NIR regions for Group No. 4 (Table 3). Due to the shift of NH_4^+ peaks in NH_4NO_3, the optimal spectral range in the 5000–4000 cm^{-1} region is obviously shifted to higher frequencies compared with those ranges in Group No. 3.

For NO_3^- determination in Groups No. 3 and 4 (Table 3), the values of R^2, SEC, SEP, and CV are quite similar, yielding 96%, 12 ppm, 13 ppm, and 6%, respectively. The number of PLS factors required are also the same for both groups in the 3400–2400 cm^{-1} region. Due to the perfect correlation between NH_4^+ and NO_3^- in NH_4NO_3 and the strong intensities of both NH_4Cl and $NaNO_3$ features in the 3400–2400 cm^{-1} region, the optimal spectral range for NO_3^- measurement of Group No. 4 has partially included both NH_4^+ and NO_3^- features compared with those spectral ranges of Group No. 3 whereas only NO_3^- features are included.

Representative concentration correlation plots for NH_4^+ measurement of Group No. 1 in the 3400–2400 cm^{-1} region and Group No. 3 in the 5000–4000 cm^{-1} region are presented in Figures 4 and 5, respectively. The fitted lines for both groups provide good agreement with the ideal one-to-one line of perfect correlation between actual and predicted NH_4^+ concentration in sand. The fitted calibration lines nearly resemble the prediction lines for both groups. The scatter of data within each sample and around the fitted lines is larger for Group No. 3 compared with Group No. 1 and this is reflected in the somewhat higher SEP for Group No. 3 compared to Group No. 1.

Marcel Dekker, Inc.
270 Madison Avenue, New York, New York 10016

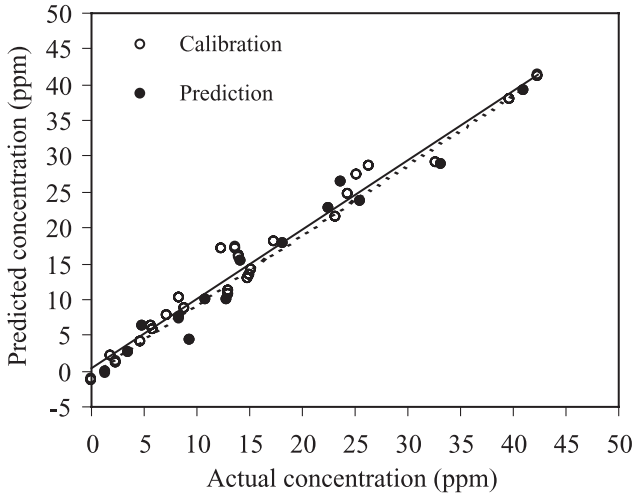

Figure 4. Concentration correlation plot for ammonium added to sand (Group No. 1) using the 3400–2400 cm^{-1} region. The solid and dashed lines indicate the fitted line based on a calibration set (solid) and a prediction set (dashed), respectively.

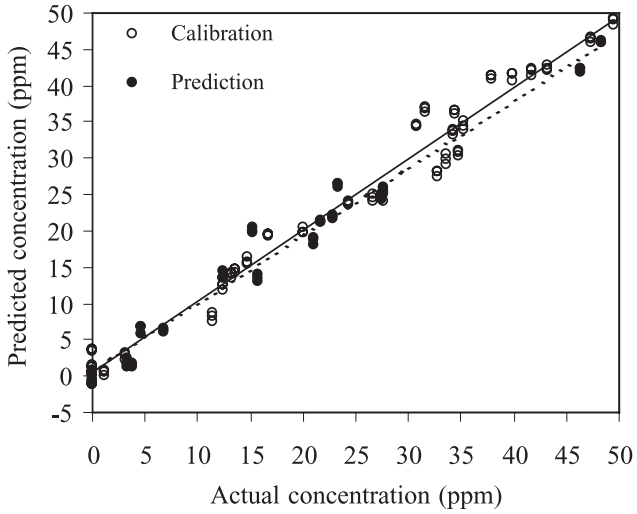

Figure 5. Concentration correlation plot for ammonium when added both ammonium and nitrate to sand (Group No. 3) using the 5000–4000 cm^{-1} region. The solid and dashed lines indicate the fitted line based on a calibration set (solid) and a prediction set (dashed), respectively.

MARCEL DEKKER, INC.
270 Madison Avenue, New York, New York 10016

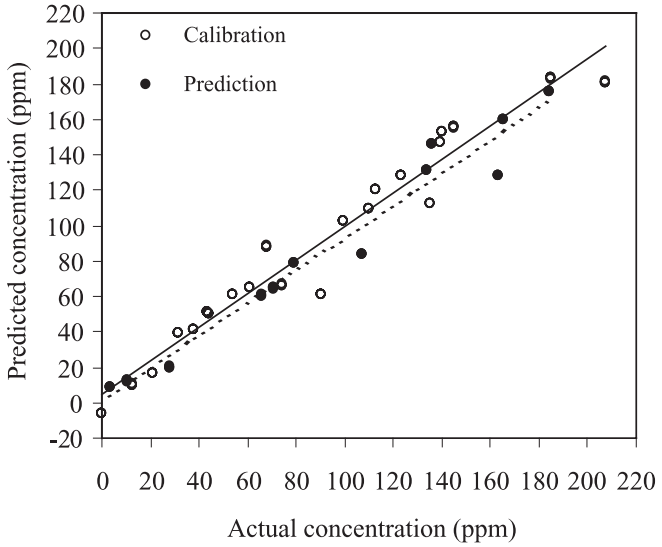

Figure 6. Concentration correlation plot for nitrate added to sand (Group No. 2) using the 3400–2400 cm^{-1} region. The solid and dashed lines indicate the fitted line based on a calibration set (solid) and a prediction set (dashed), respectively.

Figure 6 illustrates the representative concentration correlation plots for NO_3^- measurement of Group No. 2 while Figure 7 illustrates NO_3^- measurement of Group No. 3 in the 3400–2400 cm^{-1} region. The fitted calibration line differs slightly from the prediction line of Group No. 2 but no significant bias is present in either set. Both fitted lines for Group No. 3 are equivalent, however, the scatter of data within each sample and around the fitted lines is larger for Group No. 3 compared with Group No. 2. The perfect correlation between the actual and predicted NO_3^- concentration is also obtained for both groups.

The PLS parameters and outputs for NH_4^+ and NO_3^- measurements in various sized sand samples (Groups No. 5 and 6) are presented in Table 4. In Group No. 5, the results for NH_4^+ measurement are excellent for all three regions, yielding the R^2, SEC, SEP, and CV values of approximately 95%, 3 ppm, 2.5 ppm, and 4.5% respectively. Both NIR regions obtain more effective model results than does the MIR region. The 5000–4000 cm^{-1} region obtains the most effective model among the NIR regions. The measurement errors for NH_4^+ determination are approximately 2–4 times lower in Group No. 5 than those of Group No. 6 in all three regions (Table 4). In fact, the measurement errors in Group No. 5 are similar in

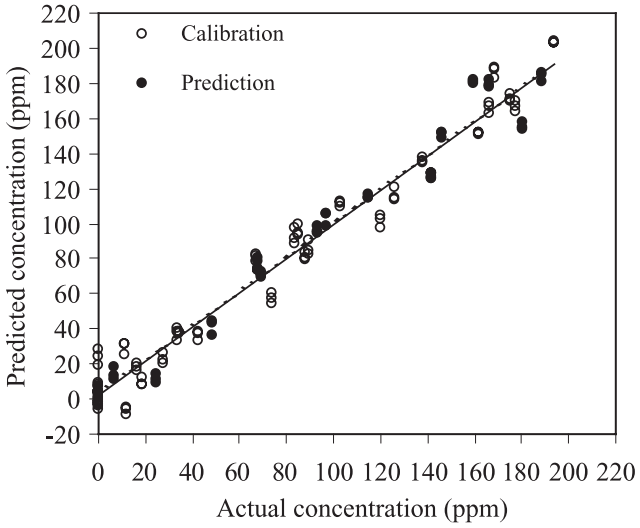

Figure 7. Concentration correlation plot for nitrate when added both ammonium and nitrate to sand (Group No. 3) using the 3400–2400 cm^{-1} region. The solid and dashed lines indicate the fitted line based on a calibration set (solid) and a prediction set (dashed), respectively.

magnitude to that obtained in Group No. 3 (Table 3) where the particle range of sand is larger than that of Group No. 5. Since the absorption intensities of NH_4Cl features in sand samples of both Groups No. 3 and 5 are somewhat equivalent (spectra not shown), similar errors would be expected. Note that the slightly lower measurement errors in Group No. 5 compared with Group No. 3 might be merely due to the larger sample sizes, approximately two times larger, which leads to more sample variations in Group No. 3 than Group No. 5.

The less effective measurements in Group No. 6 for NH_4^+ determination are likely due to the significantly lower band intensity caused by greater scattering and packing density when the sand particle size is substantially reduced. The most effective region for NH_4^+ measurement is changed from the 5000–4000 cm^{-1} region in Groups No. 3 and 5 to the region of 3400–2400 cm^{-1} in Group No. 6. Generally, the scattering coefficient is less at low wavenumbers (long wavelengths), allowing radiation to penetrate more deeply into a sample which in turn increases the absorption intensity. Thus, the NH_4Cl features would be more distinct in the MIR region than both NIR regions, resulting in lower measurement errors. The number of PLS factors for NH_4^+ measurement are essentially

Table 4. Optimal parameters and measurement errors for PLS calibrations of groups No. 5 and 6.

Spectral range (cm^{-1})	#Factors	R^2 (%)[a]	SEC (ppm)[b]	SEP (ppm)[c]	Max. concentration (ppm)[d]	Optimal range (cm^{-1})
Group No. 5: 63–106 μm						
Nitrate measurement						
3400–2400	5	98	9.71	10.03	189	2800–2650
Ammonium measurement						
3400–2400	4	94	4.47	2.75	53	2950–2590
5000–4000	4	98	2.74	1.69	53	5000–4400
6500–5500	5	99	1.98	2.46	53	6470–5800
Group No. 6: less than 53 μm						
Nitrate measurement						
3400–2400	6	95	18.75	15.89	209	2970–2400
Ammonium measurement						
3400–2400	5	96	3.94	4.4	52	2850–2500
5000–4000	5	94	4.85	6.79	52	4780–4400
6500–5500	5	93	4.85	13.67	52	6490–6000

[a]Coefficient of determination.
[b]Standard error of calibration.
[c]Standard error of prediction.
[d]Maximum concentration of analyte in the study.

equivalent in both Groups No. 5 and 6 in all regions (Table 4). The optimal spectral ranges include similar NH_4Cl features in both groups.

For NO_3^- measurement in the 3400–2400 cm^{-1} region, the results are less effective in Group No. 6 relative to Group No. 5, which would be expected for smaller particle sizes due to high scattering and over packing density, as explained previously. Despite the differences in sand particles, Group No. 5 (63–106 μm) achieves essentially equivalent measurements to Group No. 3 (212–300 μm), yielding the R^2, SEC, SEP, and CV values of approximately 98%, 10 ppm, 10 ppm, and 5.3% respectively. The slight differences in model parameters between Groups No. 3 and 5 might be due to the difference in sample sizes. The number of PLS factors for NO_3^- measurement are basically the same for Group No. 3 (Table 3) and for Groups No. 5 and 6 (Table 4). The optimal spectral range for NO_3^- measurement in Group No. 6 is larger in width than Group No. 5.

Representative correlation plots for NH_4^+ measurement using the region of 5000–4000 cm^{-1} are shown in Figures 8 and 9 for Groups No. 5 and 6, respectively. Close agreement with the one-to-one correlation lines

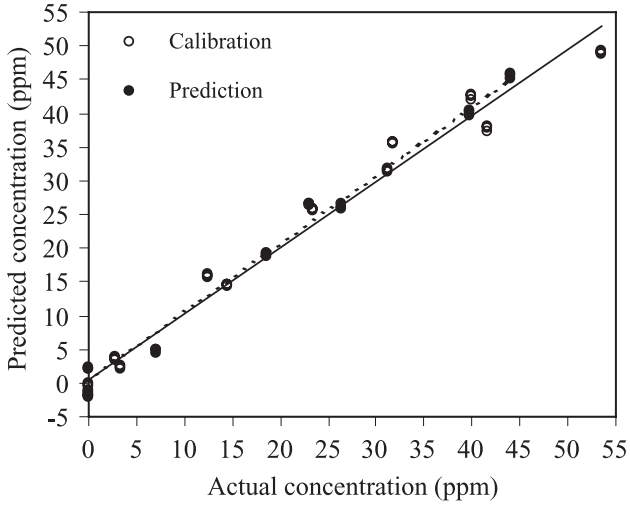

Figure 8. Concentration correlation plot for ammonium when added both nitrate and ammonium to sand (Group No. 5: 63–106 μm) using the 5000–4000 cm^{-1} region. The solid and dashed lines indicate the fitted line based on a calibration set (solid) and a prediction set (dashed), respectively.

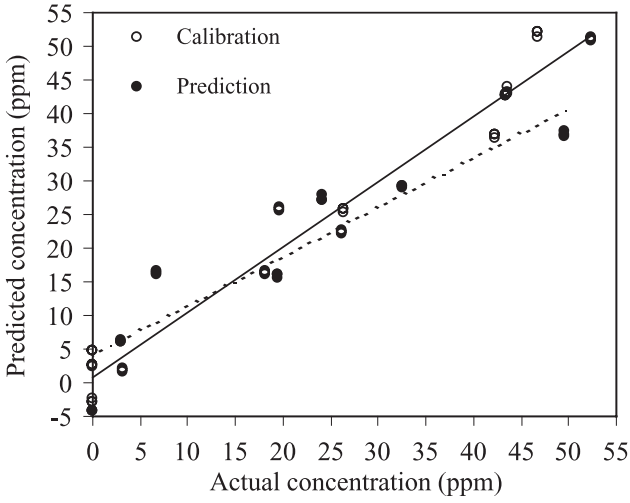

Figure 9. Concentration correlation plot for ammonium when added both nitrate and ammonium to sand (Group No. 6: less than 53 μm) using the 5000–4000 cm^{-1} region. The solid and dashed lines indicate the fitted line based on a calibration set (solid) and a prediction set (dashed), respectively.

MARCEL DEKKER, INC.
270 Madison Avenue, New York, New York 10016

of both calibration and prediction sets are achieved in Group No. 5 as for Group No. 3 (figure not shown). A representative correlation plot of Group No. 6 (Figure 9), however, indicates a significantly lower value of the slope for the prediction line than for that of the calibration line. The scatter of data around the fitted line is also larger in Group No. 6 than Group No. 5, which is reflected in the approximately three times higher SEP in the former group than the latter group.

Ammonium and Nitrate Measurements in Soil Samples

Table 5 presents the results for the measurements of NH_4^+ and NO_3^- in soil samples (Group No. 7). For NH_4^+ measurement, the MIR region of 3400–2400 cm^{-1} provides the most effective model with an R^2 of 79%. The SEC, SEP, and CV values in the MIR region are roughly 28 ppm, 34 ppm and 17%, respectively. The optimal model requires twelve PLS factors, which is relatively high but is feasible for the complex soil matrix. The linear relationship between the NH_4^+ concentrations and DRIFTS spectra was not successfully established in either NIR region (R^2<60). The measurement errors in the NIR regions are approximately two times greater than those of the MIR region. These are unexpected since the NIR regions performed as well as the MIR region for NH_4^+ measurement in sand samples, particularly in the 5000–4000 cm^{-1} region, even though the

Table 5. Optimal parameters and measurement errors for PLS calibrations of group no. 7.

Spectral range (cm^{-1})	#Factors	R^2 (%)[a]	SEC (ppm)[b]	SEP (ppm)[c]	Max. concentration (ppm)[d]	Optimal range (cm^{-1})
Group No. 7: Soil samples						
Nitrate measurement						
3400–2400	10	91	79.41	111.02	990	2720–2400
Ammonium measurement						
3400–2400	12	79	27.54	33.71	200	3300–2670
5000–4000	8	52	41.76	61.29	200	4910–4800
6500–5500	7	57	39.34	61.44	200	5790–5650

[a]Coefficient of determination.
[b]Standard error of calibration.
[c]Standard error of prediction.
[d]Maximum concentration of analyte in the study.

absorption intensity of NH_4Cl features in the MIR region is higher than the NIR regions. The optimal spectral range for NH_4^+ measurement is quite wide due to the less distinct NH_4^+ features in soil samples within the MIR region. The vibrational features of other components (including NO_3^- features) in soil samples could partly mask the NH_4Cl features, reducing the intensity of the distinct NH_4Cl features.

A strong relationship between the actual NO_3^- concentrations in soil and the DRIFTS spectra in the 3400–2400 cm^{-1} region is obtained, yielding an R^2 of 91% (Table 5). With ten PLS factors, the measurement errors are roughly 80 ppm, 110 ppm and 14% for SEC, SEP, and CV, respectively. Note that the concentration range of NO_3^- is larger than previously evaluated using sand samples. The optimal spectral range of 2720–2400 cm^{-1} includes the distinct feature of $NaNO_3$ located around 2440 cm^{-1}.

Representative correlation plots for NH_4^+ and NO_3^- measurements in soil samples using the region of 3400–2400 cm^{-1} are illustrated in Figures 10 and 11, respectively. Trend lines between actual and predicted concentration of NH_4^+ are very similar for calibration and prediction sets (Figure 10). The negative predicted NH_4^+ content might occur partly due to the high SEP value or partly due to other outliers remaining in the

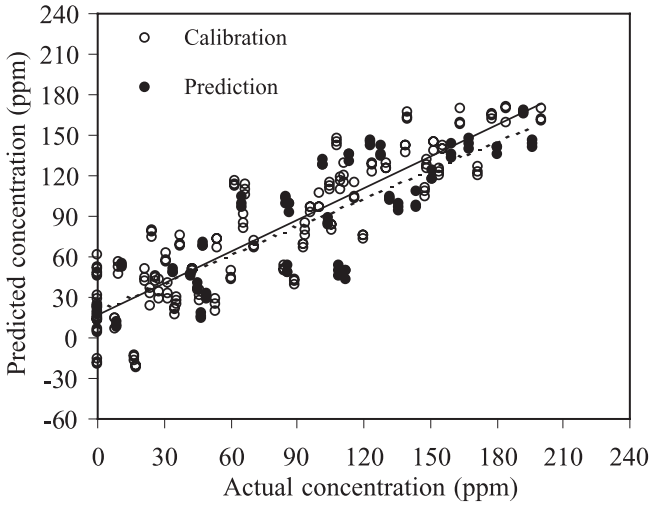

Figure 10. Concentration correlation plot for ammonium when added both nitrate and ammonium to soil (Group No. 7) using the 3400–2400 cm^{-1} region. The solid and dashed lines indicate the fitted line based on a calibration set (solid) and a prediction set (dashed), respectively.

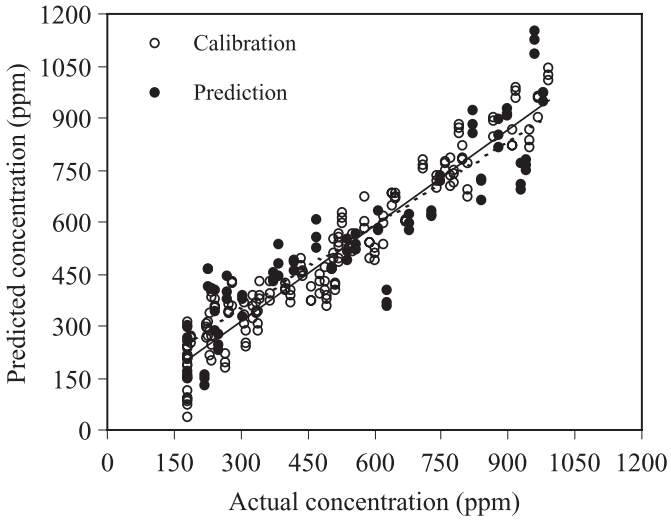

Figure 11. Concentration correlation plot for nitrate when added both nitrate and ammonium to soil (Group No. 7) using the 3400–2400 cm^{-1} region. The solid and dashed lines indicate the fitted line based on a calibration set (solid) and a prediction set (dashed), respectively.

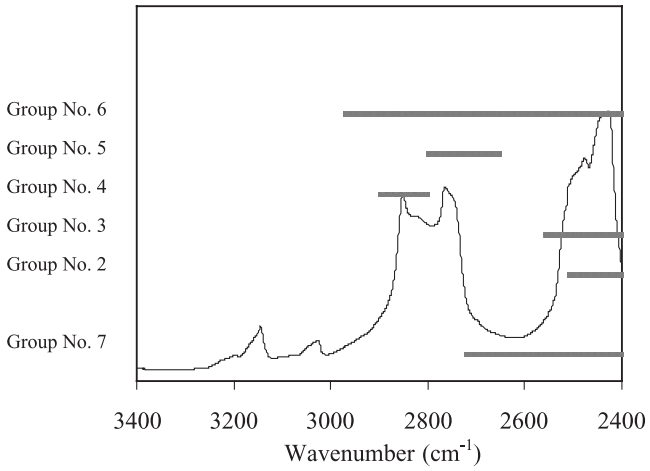

Figure 12. The optimal spectral ranges for nitrate measurement in sand (Groups No. 2, 3, 4, 5, and 6) and soil samples (Group No. 7) placed on top of a $NaNO_3$ spectrum within the 3400–2400 cm^{-1} region.

Marcel Dekker, Inc.
270 Madison Avenue, New York, New York 10016

calibration model. A good correlation is obtained for NO_3^- measurement (Figure 11). The large intercepts of both the calibration and the prediction lines are due to the high NO_3^- concentration initially presented in soil. The scatter of data around the fitted lines is greater for NH_4^+ than NO_3^- measurement, which is reflected in higher SEP of NH_4^+ measurement.

The optimal spectral ranges of the most effective models of all experimental groups for NO_3^- measurement in sand and soil samples in the MIR region of 3400–2400 cm^{-1} are shown in Figure 12. The common spectral range of all experiments for NO_3^- measurement in both sand and soil samples includes the spectral window of roughly 2900–2400 cm^{-1}. The spectral window of 2500–2400 cm^{-1} that separates the optimal range of NH_4^+ measurement from NO_3^- is the region for the distinct NO_3^- feature located around 2440 cm^{-1}.

In this study, the ability of the DRIFTS technique to quantitatively analyze mineral N (NH_4^+ and NO_3^-) was investigated. Sand was initially used as a sample matrix not only because it is the primary component in soil but also because it can be used to maintain similar physical properties permitting analysis of only variations in chemical components. The particle sizes of sand were reduced to investigate the effect of physical variations of sand while keeping similar chemical components. After studying sand samples, soil was employed as the sample matrix for the quantitative analysis of mineral N. The concentrations of NH_4^+ and NO_3^- added into soil samples are much higher than those of sand since no N features were apparent at the concentrations of 200 ppm NO_3^- and 50 ppm NH_4^+ due to the complexity of the soil matrix. The concentration ranges of 180–1000 ppm NO_3^- and 0–200 ppm NH_4^+ were employed to estimate the detection limit of the DRIFTS technique. Sand samples were not diluted with KBr while soil samples were diluted with 1 wt% in KBr matrix.

Both NIR regions (5000–4000 cm^{-1} and 6500–5500 cm^{-1}) and MIR region (3400–2400 cm^{-1}) provided good performance for NH_4^+ measurements in sand samples (212–300 μm). The MIR region was the most effective region for NO_3^- measurement in sand due to the relatively high band intensities of $NaNO_3$ compared with sand features in the MIR region. The similarity of SEP values for NH_4^+ and NO_3^- measurements in the sand samples with the particle range of 212–300 μm (Groups No. 1, 2, 3, and 4) indicates that varying only the chemical property in sand samples has a minor effect on the model efficiency. The reasons for good measurements of NH_4^+ and NO_3^- in this sand matrix were partly due to the uniformity and homogeneity of the sample matrix and partly due to the more intense features of NH_4Cl and $NaNO_3$ compared with that of the sand matrix. The spectral ranges selected for each analyte were quite different between three calibration sets in some cases even though the measurement errors were

similar. Instrument variations and collection variability such as noise, source intensity, and temperature might account for the differences among samples in each calibration set.

In samples with consistent chemical components but varying physical properties such as a reduced particle size (Groups No. 3, 5, and 6) the SEP values for NH_4^+ measurement were significantly increased. The SEP was larger by approximately 2–4 times when the sand particles were reduced to less than 53 μm (Group No. 6). The MIR region was the most effective region for both NH_4^+ and NO_3^- measurements in sand with the smallest particle sizes (Group No. 6).

When soil was used as the sample matrix, an increase in measurement errors was expected due to the complexity of soil components. With CV values of 17% and 14% within the concentration range of 0–200 ppm NH_4^+ and 180–1000 ppm NO_3^-, the optimal models for the measurements of NH_4^+ and NO_3^- in soil are somewhat effective but have room for improvement. Both NIR regions failed to provide good calibrations for NH_4^+ measurement in soil samples. A possible explanation for the low performance in the NIR might be due to the stronger features of other components in soil or to the high NO_3^- content. Humic substances in soil are likely to play a role in masking the measurements (data not shown).

CONCLUSIONS

Measurement of the low concentration of mineral N (NH_4^+ and NO_3^-) in sand by the DRIFTS method was investigated. The concentration ranges of 0–50 ppm as NH_4^+ and 0–200 ppm as NO_3^- are appropriate for desert soils. Results show that both NIR and MIR regions are very effective for NH_4^+ determination in sand samples. For NO_3^- determination, the MIR region was substantially more useful than those of NIR regions. On the average, the detection limits, calculated based on three times the SEP, for the measurements of NH_4^+ and NO_3^- when changing only chemical components in sand are 9 ppm NH_4^+ and 39 ppm NO_3^-, respectively. The MIR region provides the most effective model for both NH_4^+ and NO_3^- measurements in the highly scattering sand matrix (particle sizes less than 53 μm), yielding detection limits of 15 ppm NH_4^+ and 50 ppm NO_3^-.

The MIR region performs reasonably well for the prediction of NH_4^+ and NO_3^- concentrations in the Pima clay loam soil samples with the concentration range of 0–200 ppm NH_4^+ and 180–1000 ppm NO_3^-. Both NIR regions failed to predict the concentrations of NH_4^+ and NO_3^- in soil.

Marcel Dekker, Inc.
270 Madison Avenue, New York, New York 10016

The detection limits for the prediction of NH_4^+ and NO_3^- in soil within the MIR region are roughly 100 ppm NH_4^+ and 330 ppm NO_3^-.

The effective spectral ranges for NH_4^+ and NO_3^- measurements using sand and soil samples are within the MIR regions of 3000–2500 cm^{-1} and 2900–2400 cm^{-1}, respectively. The spectral range of 2500–2400 cm^{-1} includes the distinct feature of NO_3^- that is visible in sample spectra at high concentrations. This spectral range could be used for NO_3^- measurement in portable DRIFTS equipment because it includes the distinct feature of NO_3^- that is less influenced by variations of other properties in soil sample and also requires narrow spectral width.

REFERENCES

1. Barber, S.A. *Soil Nutrient Bioavailability: A Mechanistic Approach*, 2nd Ed.; John Wiley & Sons, Inc.: New York, 1995; 180 pp.
2. Petit, S.; Righi, D.; Madejova, J.; Decarreau, A. Interpretation of the infrared NH_4^+ spectrum of the NH_4^+-clays: application to the evaluation of the layer charge. Clay Miner. **1999**, *34* (4), 543–549.
3. Krohn, M.D.; Altaner, S.P. Near-infrared detection of ammonium minerals. Geophysics **1987**, *52* (7), 924–930.
4. Ehsani, M.R.; Upadhyaya, S.K.; Slaughter, D.; Shafii, S.; Pelletier, M. A NIR technique for rapid determination of soil mineral nitrogen. Precis. Agric. **1999**, *1* (2), 217–234.
5. Vogt, R.; Finlayson-Pitts, B.J. A diffuse reflectance infrared Fourier transform spectroscopic (DRIFTS) study of the surface reaction of NaCl with gaseous NO_2 and HNO_3. J. Phys. Chem. **1994**, *98* (14), 3747–3755.
6. Janik, L.J.; Merry, R.H.; Skjemstad, J.O. Can mid infrared diffuse reflectance analysis replace soil extractions? Aust. J. Exp. Agric. **1998**, *38* (7), 681–696.
7. Dalal, R.C.; Henry, R.J. Simultaneous determination of moisture, organic carbon, and total nitrogen by near infrared reflectance spectrophotometry. Soil Sci. Soc. Am. J. **1986**, *50* (1), 120–123.
8. Morra, M. J.; Hall, M. H.; Freeborn, L. L. Carbon and nitrogen analysis of soil fractions using near-infrared reflectance spectroscopy. Soil Sci. Soc. Am. J. **1991**, *55* (1), 288–291.
9. Reeves, J.B., III; McCarty, G.W.; Meisinger, J.J. Near infrared reflectance spectroscopy for the analysis of agricultural soils. J. Near Infrared Spectrosc. **1999**, *7* (3), 179–193.
10. Krischenko, V.P.; Samokhvalov, S.G.; Fomina, L.G.; Novikova, G.A. Use of infrared spectroscopy for the determination of some properties

MARCEL DEKKER, INC.
270 Madison Avenue, New York, New York 10016

of soil. In *Making Light Work: Advances in Near Infrared Spectroscopy*; Murray, I., Cowe, I.A., Eds.; Ian Michael Publications: West Sussex, UK, 1992; 239–249.
11. Janik, L.J.; Skjemstad, J.O. Characterization and analysis of soils using mid-infrared partial least squares: II. Correlations with some laboratory data. Aust. J. Soil Res. **1995**, *33* (4), 637–650.
12. Reeves, J.B., III; McCarty, G.W.; Reeves, V.B. Mid-infrared diffuse reflectance spectroscopy for the quantitative analysis of agricultural soils. J. Agric. Food Chem. **2001**, *49* (2), 766–772.
13. Sims, J.R.; Jackson, G.D. Rapid analysis of soil nitrate with chromotropic acid. Soil Sci. Soc. Am. Proc. **1971**, *35* (4), 603–606.
14. Smith, B.C. *Infrared Spectral Interpretation: A Systematic Approach*; CRC Press: Boca Raton, FL, 1999; 14 pp.
15. Martens, H.; Naes, T. *Multivariate Calibration*; John Wiley & Sons, Inc.: New York, 1989; 73 pp.

Received January 7, 2003
Accepted May 4, 2003